In order to provide a simple correction for the response of the MOSFET detector to various LET effects, we employed a method originally used to correct imaging plate response.[14] A Bragg curve was obtained using the IC detector to establish a standard for the proton beam depth-dose distribution. This curve was then used to calculate correction factors (IC/MOSFET) as a function of proton penetration depth.

The proton penetration depth can be considered as a residual range. Since the protons at any point have a variety of energies due to multiple scattering effects, the residual proton range at an arbitrary point may be calculated using the pencil beam dose calculation algorithm (PBA),[15-17] in which the pencil beam dose distribution is separated into a central-axis term and an off-axis term. The central-axis term represents the measured depth-dose distribution of the broad beam. The off-axis term is a two-dimensional Gaussian distribution the standard deviation of which corresponds to the lateral beam spread. The dose $F(x, y, z, (x_0, y_0))$ delivered by a single pencil beam at an entrance position (x_0, y_0) is given by:

$$F(x,y,z;(x_0,y_0)) = \phi(x_0,y_0)DD(z;(x_0,y_0)) \times \frac{1}{2\pi\sigma(z)^2}\exp\left(-\frac{(x_0-x)^2-(y_0-y)^2}{2\sigma(z)^2}\right), \quad (2)$$

where $\phi(x_0,y_0)$ is the intensity profile of the broad beam, $DD(z;(x_0,y_0))$ is the depth-dose distribution of the broad beam, and $\sigma(z)$ is the proton spread due to multiple scattering effects in the bolus and polyethylene slabs and the configuration of the beam line at z. We can obtain the dose distribution in the region of interest by generating many pencil beams and summing their dose distributions. For dose distributions of protons traversing an L-shaped phantom, Kohno et al.[16] reported the precision of doses calculated using the PBA is approximately 2.5%. The PBA may therefore be considered a precise and practical method for calculating the proton residual range in order to obtain correction factors at arbitrary locations.

The correction factor for the MOSFET response CF(x,y,z) is given by:

$$CF(x,y,z) = \frac{\sum_{i=1}^{n} cf_{dd}(z;(x_i,y_i))F(x,y,z;(x_i,y_i))}{\sum_{i=1}^{n} F(x,y,z;(x_i,y_i))} \quad (3)$$

in which i is the ith pencil beam, n is the total number of pencil beams, (x_i,y_i) is the position of a generated pencil beam, and $cf_{dd}(z;(x_i,y_i))$ is $cf_{mono}(z = d_{PE})$ or $cf_{SOBP}(z = d_{PE})$ (as described in Section B.4 above). The dose measured by the MOSFET detector at (x,y,z), D(x,y,z) may be calculated using:

$$D(x,y,z) = CF(x,y,z) \cdot D_{raw}(x,y,z), \quad (4)$$

where $D_{raw}(x,y,z)$ is the raw dose (as described in Section B.2 above).

Proton dose distributions resulting from an L-shaped bolus (Fig. 1) were measured using the MOSFET and the IC detectors. Protons passing near the abrupt change in thickness at x = 0 displayed a range of energies due to multiple scattering effects, and it was necessary to calculate the proton residual range using the PBA in order to obtain the correction factor.

III. RESULTS & DISCUSSION

A. Dose sensitivity

The sensitivity of the TN-252RD MOSFET detector was 0.72 ± 0.01 (mV/cGy) and the corresponding reproducibility was ± 1.4%. Although the sensitivity of this detector was lower than the TN-502RD MOSFET with a thicker oxide layer, its reproducibility was within 2%. Figure 2 is a graph of the TN-252RD MOSFET sensitivity for each proton energy value. The sensitivities to 150, 157, and 200 MeV proton beams were almost identical, but the sensitivity was reduced at lower proton energies of 100 and 50 MeV.

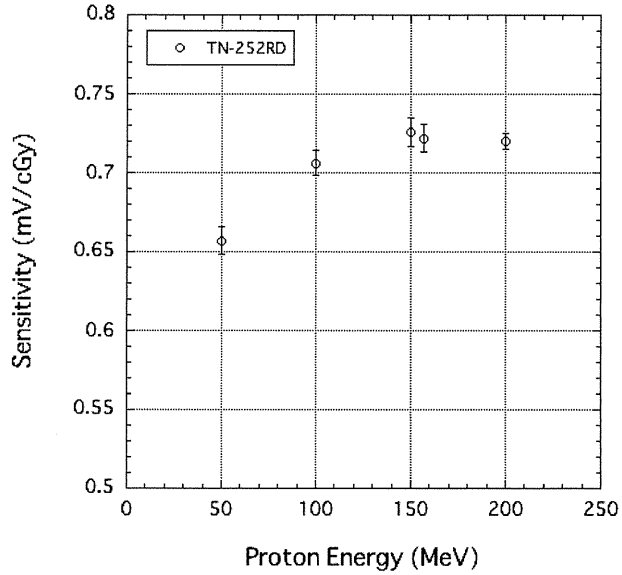

FIG. 2. MOSFET sensitivity for 200, 157, 150, 100 and 50 MeV proton beams.

B. Angular dependence

Figure 3 depicts an angular dependence of the MOSFET detector exposed to a 190 MeV proton beam, and the correction value for the angular response of the MOSFET detector. The electric field is parallel to the incident proton beam when the MOSFET detector is mounted at 0 degrees. The response was normalized to 0°, corresponding to a beam perpendicular to the MOSFET encapsulation epoxy. The angular response at 180° agreed well with the 0° measurements (within ± 2.0%). The TN-252RD detector displayed a maximum overresponse of +9.0%. The overresponse occurs because the fraction of charge pairs escaping recombination increases at larger angles between the electric field and the proton track.[18] Despite the large value, this is a dramatic improvement of almost 10% relative to the TN-502RD device,[7] suggesting that MOSFET detectors constructed using thinner SiO_2 layers exhibit reduced angular dependence. The correction value $CV_{Ang}(\theta)$ may be obtained from the angular response of the TN-252RD detector at a beam angle θ using the relation:

$$CV_{Ang}(\theta) = 1 - 0.00197 \cdot \theta + 0.0000109 \cdot \theta^2. \quad (5)$$

Using this correction value, we can correct the angular response of the TN-252RD MOSFET detector to within 1.5%.

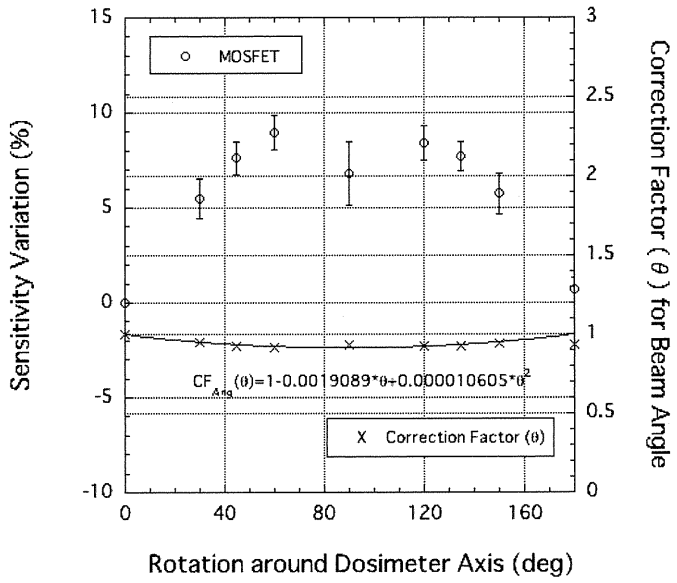

FIG. 3. Angular dependence of MOSFET detectors exposed to a 190 MeV proton beam. The correction value for the angular response of the MOSFET detector is also plotted.

C. Depth-dose curves

Figure 4 shows a comparison of Bragg curves obtained using IC and MOSFET detectors at high-bias setting for a 190 MeV proton beam, and the correction factor for the response of the MOSFET detector was calculated as a function of proton penetration depth. The relative response of the TN-252RD MOSFET detector at the Bragg peak was 0.74. This response relative to the TN-502RD detector[7] also is a larger than a 10% improvement. The correction factor $cf_{mono}(z = d_{PE})$ for the response of the MOSFET detector was determined as a function of proton penetration depth as follows:

$$cf_{mono}(d_{PE}) = \begin{cases} 1 & [d_{PE} < 100.421\,(mm)] \\ 0.781885 + 0.002172 \cdot d_{PE} & [100.421\,(mm) \le d_{PE} < 154.784\,(mm)] \\ -2.94139 + 0.0262266 \cdot d_{PE} & [154.784\,(mm) \le d_{PE}] \end{cases} \quad (6)$$

The MOSFET with the correction agreed well with the IC within 1.5%, as shown in Fig. 4.

A comparison of the SOBP obtained using the IC and MOSFET detectors is shown in Fig. 5. Figure 5 also shows the correction factor for the response of the MOSFET detector was calculated as a function of proton penetration depth. The ratio of the IC and MOSFET (IC/MOSFET) response was also obtained. The correction factor $cf_{SOBP}(d_{PE})$ was expressed as a function of PE thickness using:

$$cf_{SOBP}(d_{PE}) = \begin{cases} 1 & [d_{PE} < 40\,(mm)] \\ 0.94639 + 0.00134025 \cdot d_{PE} & [40\,(mm) \le d_{PE} < 140\,(mm)] \\ 6.59257 - 0.0793194 \cdot d_{PE} + 0.00028807 \cdot d_{PE}^{\,2} & [140\,(mm) \le d_{PE}] \end{cases} \quad (7)$$

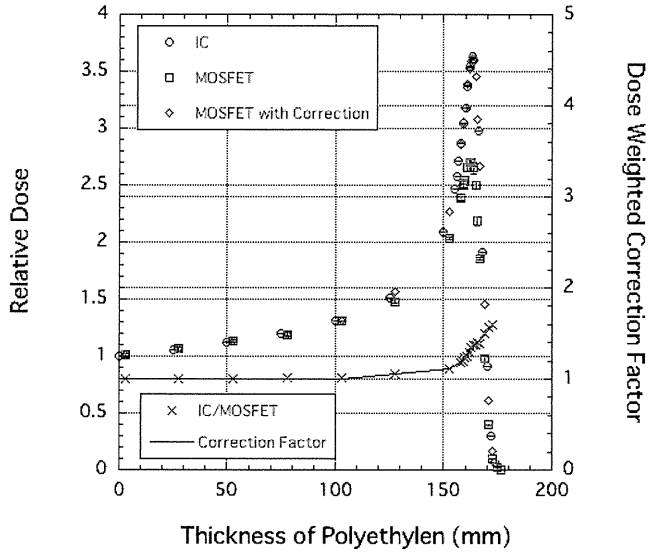

FIG. 4. Comparison of Bragg curves obtained using IC and MOSFET detectors at high-bias setting for a 190 MeV proton beam. The correction factor for the response of the MOSFET detector was calculated as a function of proton penetration depth.

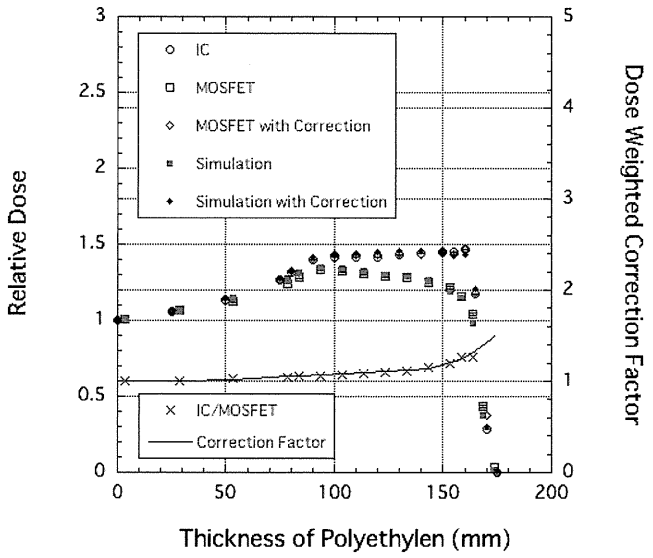

FIG. 5. Comparison of SOBP obtained using IC and MOSFET detectors. The correction factor for the response of the MOSFET detector was calculated as a function of proton penetration depth.

The MOSFET with the correction agreed well with the IC within 1.4%, as shown in Fig. 5.

In this method, $cf_{SOBP}(d_{PE})$ must be measured and calculated for each SOBP width. However, a SOBP distribution may be obtained in a stepwise manner from the dose contributions of mono-energetic proton beams traversing the individual elements of the ridge filter. For example, the "Simulation" curve in Fig. 5 depicts the SOBP distribution obtained using the

uncorrected depth-output curve measured with the MOSFET detector. The "Simulation with Correction" curve depicts results corrected without the necessity of applying the experimentally determined MOSFET response corrections to the "Simulation" curve. Thus, given $cf_{mono}(d_{PE})$ of Eq. (6) for the mono-energetic proton beam, we can obtain $cf_{SOBP}(d_{PE})$ for various SOBP-width proton beams by simulating the SOBP beam using the Bragg curve of a mono-energetic proton beam.

D. Bolus experiments

Figure 6 compares the lateral dose distributions obtained for a 190 MeV proton beam using IC and MOSFET detectors at PE thicknesses of 0 (a), 100 (b), 105 (c), 110 (d) and 115 (e) mm. The error bar in Fig. 6 includes the reproducibility of the MOSFET measurements and calculation errors of 3% to account for uncertainties in the PBA (as described in Materials and Methods Section C.2). In Fig. 6(a), a bump and dip structure is evident near x = 0. This is the result of edge scattering effects due to the abrupt change in thickness. The uncorrected MOSFET results agreed well with the IC measurements, and the MOSFET response due to LET did not change at this depth. Thus, in shallow regions, depth-dose distribution corrections are unnecessary.

On the other hand, the MOSFET detector response began to change at $x < 0$ and the uncorrected MOSFET output deviated significantly from the IC response (Fig. 6(b)). Because the depth at $x < 0$ is close to the Bragg peak position, the MOSFET response was reduced. Since edge scattering causes the lateral dose distribution near x = 0 to be determined by protons with a distribution of energies, we expected that changes in the MOSFET response would be complex. However, the corrected output of the MOSFET detector agreed well with the IC results within an average difference of 4.4%, demonstrating that MOSFET detectors are suitable for proton dosimetry when the response is corrected. Despite the drastic change in MOSFET detector response near $x < 0$ for PE thicknesses of 105, 110 and 115 mm, the corrected output agreed with the IC results (Figs. 6(c), 6(d), and 6(e)) within 3.2% (1 sigma).

Figure 7 is a comparison of the lateral-dose distribution obtained using the IC and MOSFET detectors at PE thicknesses of 0 (a), 50 (b) and 100 (c) mm for an SOBP proton beam. The corrected MOSFET output agreed well with the IC results. For the SOBP beam, the accuracy of the dose measurement was approximately 2.3% (1 sigma).

By employing correction methods for LET and angular dependence, it is possible to perform *in vivo* proton dosimetry using a MOSFET detector. However, the correction method for LET effects is highly dependent on the precision of the PBA calculation, and further improvements to the dose calculation algorithm (for instance the application of Monte Carlo methods) would be desirable in situations involving tissues with significant heterogeneity.[19-23]

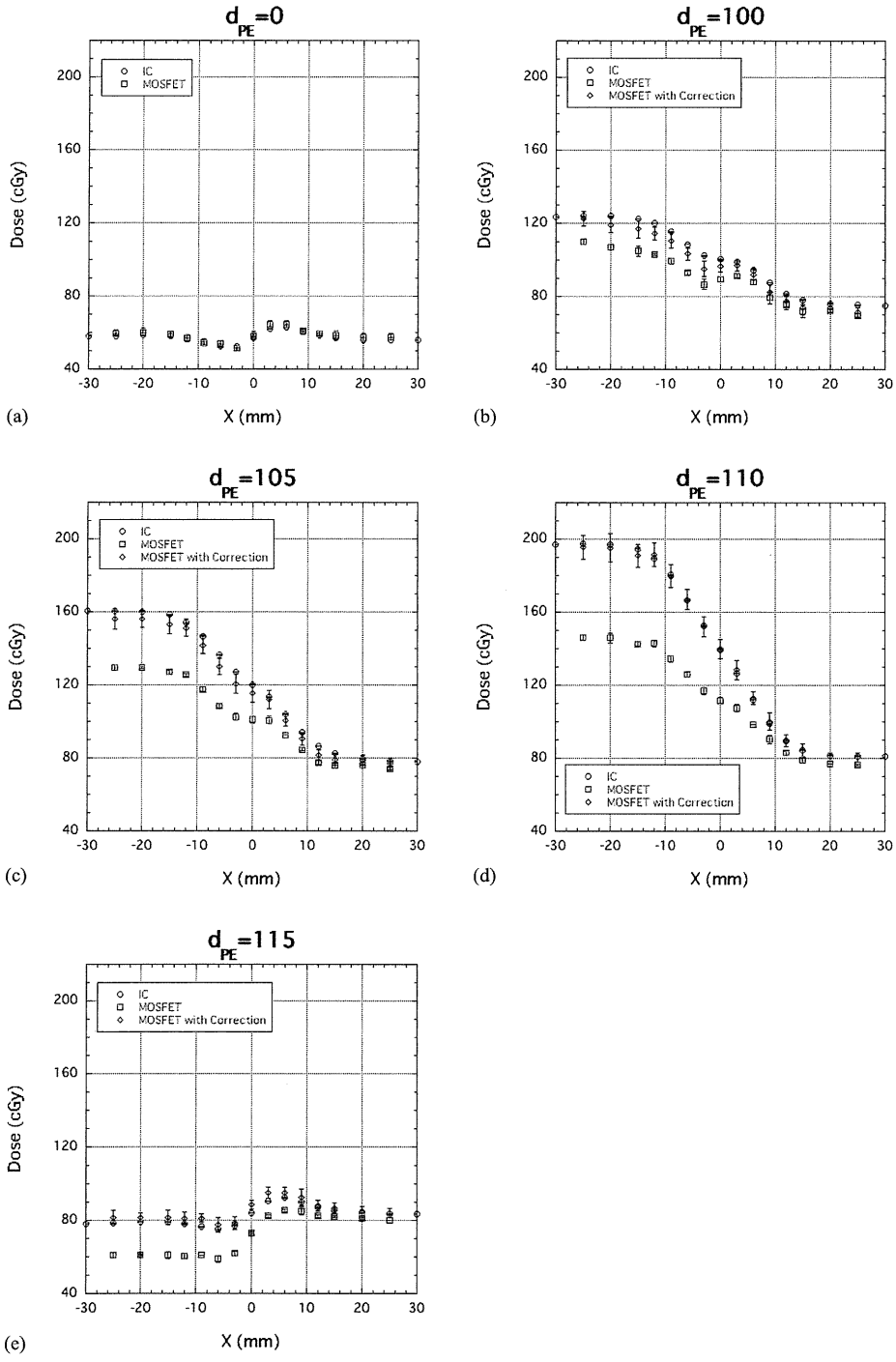

FIG. 6. Comparison of lateral-dose distribution obtained using IC, uncorrected MOSFET (MOSFET) and corrected MOSFET detectors (MOSFET with Correction) at PE thicknesses of 0 (a), 100 (b), 105 (c), 110 (d) and 115 (e) mm for a 190 MeV mono-energetic proton beam.

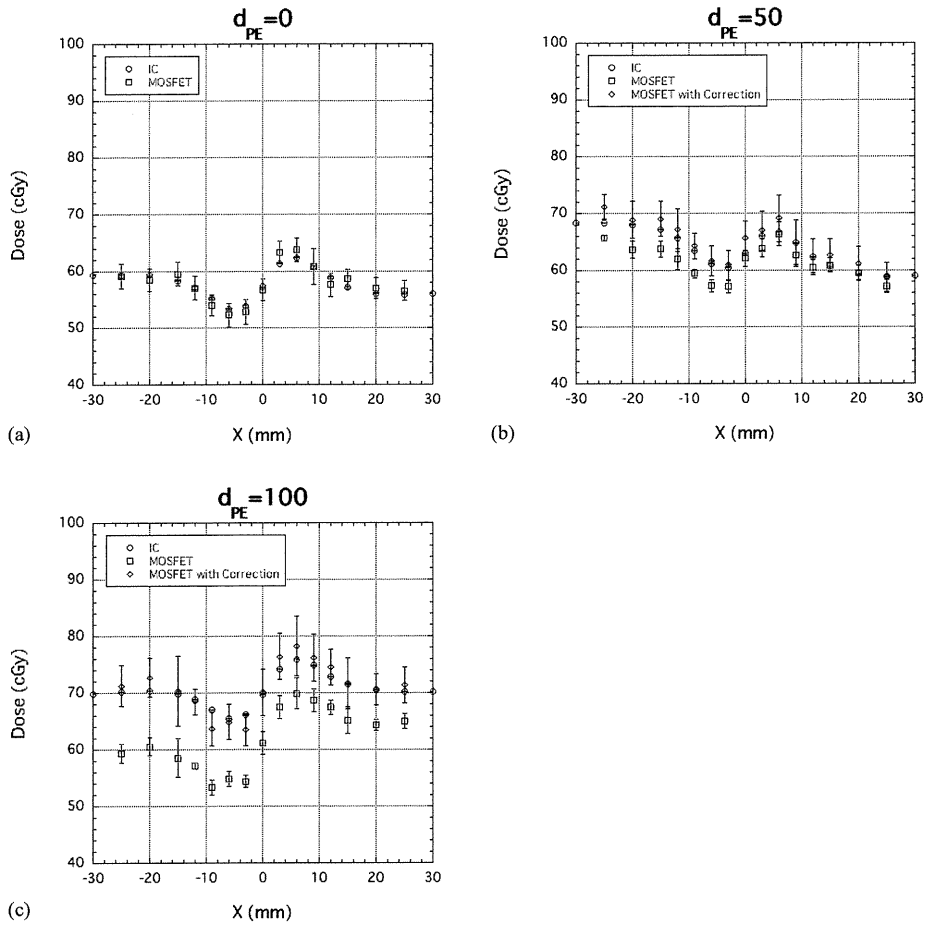

FIG. 7. Comparison of lateral-dose distribution measurements obtained using IC, uncorrected MOSFET (MOSFET) and corrected MOSFET detectors (MOSFET with Correction) at PE thicknesses of 0 (a), 50 (b) and 100 (c) mm for a SOBP proton beam.

IV. CONCLUSIONS

We experimentally evaluated the proton beam dose reproducibility, angular dependence and depth-dose relationships for a new TN-252RD MOSFET detector at high-bias voltages. The reproducibility of the MOSFET detector was within 2%, and the angular dependence was less than 9%. For depth-dose distribution measurements, the relative response of the MOSFET detector at the Bragg peak region was 26% lower than measurements obtained using an ionization chamber. A thinner oxide layer thickness improved the LET dependence in proton dosimetry, although LET dependence was still the limiting factor in accurate depth-dose estimation.

In order to measure dose distributions using a MOSFET detector, we developed a practical method for correcting the MOSFET response to proton beams. For dose distributions resulting from protons passing through an L-shaped bolus, the corrected MOSFET dose agreed well with the IC results. Absolute proton dosimetry was performed using MOSFET detectors with a precision of approximately 3% (1 sigma), and from this we conclude that it is possible to measure proton doses using MOSFET detectors.

ACKNOWLEDGMENTS

We thank Dr. A. Hallil, Best Medical Canada, for his support in the form of materials and special prototypes. We are grateful to Kazutomo Matsumura, Hideki Saitoh, Toshinobu Sasano, Naoya Uzawa and Ryuichi Oota, SHI Accelerator Service Ltd, for experimental support. The authors wish to thank Akihiro Nohtomi, Ph.D. for a critical review of the manuscript. This work was supported in part by a Grant-in-Aid for Young Scientists (B) No. 21791236 from the Japan Society for Promotion of Science (JSPS).

REFERENCES

1. Chuang CF, Verhey LJ, Xia P. Investigation of the use of MOSFET for clinical IMRT dosimetric verification. Med Phys. 2002;29(6):1109–15.
2. Ramaseshan R, Kohli KS, Zhang TJ, et al. Performance characteristics of a microMOSFET as an in vivo dosimeter in radiation therapy. Phys Med Biol. 2004;49(17):4031–48.
3. Ehringfeld C, Schmid S, Poljanc K, Kirisits C, Aiginger H, Georg D. Application of commercial MOSFET detectors for in vivo dosimetry in the therapeutic x-ray range from 80 kV to 250 kV. Phys Med Biol. 2005;50(2):289–303.
4. Bloemen-van Gurp EJ, Minken AWH, Mijnheer BJ, Dehing-Oberve CJ, Lambin P. Clinical implementation of MOSFET detectors for dosimetry in electron beams. Radiother Oncol. 2006;80(3):288–95.
5. Kohno R, Hirano E, Nishio T, et al. Dosimetric evaluation of a MOSFET detector for clinical application in photon therapy. Radiol Phys Technol. 2008;1(1):55–61.
6. Kohno R, Hirano E, Kitou S, et al. Evaluation of the usefulness of a MOSFET detector in an anthropomorphic phantom for 6-MV photon beam. Radiol Phys Technol. 2010;3(2):104–12.
7. Kohno R, Nishio T, Miyagishi T, et al. Experimental evaluation of a MOSFET dosimeter for proton dose measurements. Phys Med Biol. 2006;51(23):6077–86.
8. Cheng CW, Wolanski M, Zhao Q, et al. Dosimetric characteristics of a single use MOSFET dosimeter for in vivo dosimetry in proton therapy. Med Phys. 2010;37(8):4266–73.
9. Soubra M, Cygler J, Mackay G. Evaluation of a dual bias dual metal oxide-silicon semiconductor field effect transistor detector as radiation dosimeter. Med Phys. 1994;21(4):567–72.
10. Wang B, Kim CH, Xua XG. Monte Carlo modeling of a high-sensitivity MOSFET dosimeter for low- and medium-energy photon sources. Med Phys. 2004;31(5):1003–08.
11. Nishio T, Kataoka S, Tachibana M, et al. Development of a simple control system for uniform proton dose distribution in a dual-ring double scattering method. Phys Med Biol. 2006;51(5):1249–60.
12. Kohno R, Nishio T, Miyagishi T, et al. Evaluation of daily quality assurance for proton therapy at National Cancer Center Hospital East. Jap J Med Phys. 2006;26:153–62.
13. International Commission on Radiation Units and Measurements (ICRU). ICRU Report 49: Stopping power and ranges for protons and alpha particles. Bethesda, MD: ICRU; 1993.
14. Kohno R, Nohtomi A, Takada Y, Terunuma, T, Sakae T, Matsumoto K. A compensating method of an imaging plate response to clinical proton beams. Nucl Instr Meth Phys Res. A. 2002;481(1-3):669–74.
15. Hong L, Goitein M, Bucciolini M, et al. A pencil beam algorithm for proton dose calculations. Phys Med Biol. 1996;41(8):1305–30.
16. Kohno R, Takada Y, Sakae T, Nohtomi A, Terunuma T, Yasuoka K. Experimental evaluation of pencil beam algorithm by measurements of dose distributions of protons traversing an L-shaped phantom. Jpn J Appl Phys. 2001;40:441–45.
17. Kohno R, Takada Y, Sakae T, et al. A range-modulated pencil beam algorithm for proton dose calculations. Jpn J Appl Phys. 2001;40:5187–93.
18. Tallon RW, Kemp WT, Ackermann MR, Owen MH, Hoffland AH. Radiation damage in MOS transistors as a function of the angle between an applied electric field and various incident radiations (protons, electrons, and Co-60 gamma rays). IEEE Trans Nucl Sci. 1987;34(6):1208–13.
19. Kohno R, Sakae T, Takada Y, et al. Simplified Monte Carlo dose calculation for therapeutic proton beams. Jpn J Appl Phys. 2002;41:L294–L297.
20. Kohno R, Takada Y, Sakae T, et al. Experimental evaluation for validity of simplified Monte Carlo method in proton dose calculations. Phys Med Biol. 2003;48(10):1277–88.
21. Hotta K, Kohno R, Takada Y, et al. Improved dose-calculation accuracy in proton treatment planning using a simplified Monte Carlo method verified with three-dimensional measurements in an anthropomorphic phantom. Phys Med Biol. 2010;55(12):3545–56.
22. Aso T, Kimura S, Tanaka S, et al. Verification of the dose distributions with GEANT4 simulation for proton therapy. IEEE Trans Nucl Sci. 2005;52(4):896–901.
23. Paganetti H, Jiang H, Parodi K, Slopsema R, Engelsman M. Clinical implementation of full Monte Carlo dose calculation in proton beam therapy. Phys Med Biol. 2008;53(17):4825–53.

Diseases of the Esophagus (2010) ••, ••–••
DOI: 10.1111/j.1442-2050.2010.01141.x

DISEASES OF THE ESOPHAGUS

Original article

Submucosal tumor appearance is a useful endoscopic predictor of early primary-site recurrence after definitive chemoradiotherapy for esophageal squamous cell carcinoma

C.-H. Tu,[1] M. Muto,[2] T. Horimatsu,[2] K. Taku,[3] T. Yano,[4] K. Minashi,[4] M. Onozawa,[5] K. Nihei,[5] S. Ishikura,[5] A. Ohtsu,[4] S. Yoshida[4]

[1]*Division of Gastroenterology and Hepatology, Department of Internal Medicine, Far Eastern Memorial Hospital, Taipei, Taiwan; and* [2]*Department of Gastroenterology and Hepatology, Kyoto University, Kyoto, Japan, and* [3]*Division of Gastrointestinal Oncology, Shizuoka Cancer Center, Shizuoka, Japan,* [4]*Division of Digestive Endoscopy and Gastrointestinal Oncology, National Cancer Center Hospital East, Kashiwa, Japan, and* [5]*Division of Radiation Oncology, National Cancer Center Hospital East, Kashiwa, Japan*

SUMMARY. **Chemoradiotherapy (CRT) for esophageal cancer is disadvantageous because of a high locoregional failure rate. Detecting early small recurrent cancers at the primary site is necessary for potential salvage treatment. However, most endoscopists are inexperienced and therefore, a role for surveillance endoscopy after complete remission (CR) has not been established. We retrospectively evaluated serial surveillance endoscopic images from patients eventually proved to have primary-site recurrence in order to identify useful endoscopic features for early diagnosis. From January 2000 to December 2004, 303 patients with esophageal squamous cell carcinoma underwent definitive CRT, and 133 of them achieved CR. The surveillance endoscopic images stored at intervals of 1–3 months for the 16 patients with recurrence only at the primary tumor site and the 61 patients with no recurrence were collected for reexamination. Among 133 patients who achieved CR, 16 (12%) developed only local recurrence at the primary site. Thirteen of the 16 primary-site recurrent tumors (81%) appeared as submucosal tumors (SMT), with the remaining appearing as erosions or mild strictures. Of biopsy-proven recurrences, 81% were preceded by newly developed lesions such as SMT, erosions, or mild strictures detected by earlier surveillance endoscopies. For all 77 patients achieving CR with no metastasis, 86% of the evolving SMT with negative biopsies were eventually confirmed as cancer at later endoscopies. Thirteen of the 21 evolving lesions were subsequently confirmed as recurrent cancer. Early primary-site recurrence of esophageal cancer after a complete response to CRT is detectable with frequent endoscopic surveillance. SMT appearance is a useful endoscopic sign of early recurrence, as well as a predictor of subsequent diagnosis of recurrence.**

KEY WORDS: **chemoradiotherapy, esophageal cancer, recurrence, surveillance.**

INTRODUCTION

Definitive chemoradiotherapy (CRT) is widely accepted as a standard treatment option in the management of locally advanced esophageal cancer because of its high response rate and significant survival benefit.[1,2] A major drawback to this nonsurgical approach is locoregional treatment failure. At least 40% of patients undergoing CRT experienced local failure, some of whom did not develop distant metastases.[1,3–5]

These primary-site recurrence patients are traditionally managed with salvage esophagectomy for a chance of long-term survival, particularly in those with an earlier pathological stage (T1N0 and T2N0).[6,7] However, high perisurgical mortality and morbidity rates are major concerns.[7,8] Recently developed nonsurgical techniques, such as salvage endoscopic mucosal resection and photodynamic therapy,

Address correspondence to: Dr Manabu Muto, MD PhD, Department of Gastroenterology and Hepatology, Kyoto University, 54 Kawaharacho, Shogoin, Sakyo-ku, Kyoto 606-8507, Japan. Email: mmuto@kuhp.kyoto-u.ac.jp
List of presentations: Nil.
Author's disclosure of potential conflict of interest: The authors have no potential conflicts of interest.

have the advantages of greater safety and fewer treatment-related sequelae, while conferring promising survival benefits for local failures after definitive CRT.[9,10] Technically, endoscopic mucosal resection and photodynamic therapy are feasible only when the volume of the locally recurrent tumor is small enough to be amenable to these endoscopy-based procedures. Therefore, the application of these newer treatments depends crucially on the ability to identify early recurrent tumors by endoscopy.

A strategy of frequent surveillance endoscopy initiated early after remission of the cancer should theoretically improve the chances of detecting primary-site recurrent tumors in their early stages. This requires the prompt recognition of minute tumors arising from the former neoplastic bed, instead of from the uninvolved normal esophageal mucosa. However, the complete regression of cancer cells results in residual fibrosis, radiation-induced tissue injury, and the distortion of normal microstructures,[11,12] which may render relapsing neoplastic growth morphologically different from typical primary tumors. Apparently, most endoscopists are inexperienced in hunting for these difficult lesions. To our knowledge, no study of the skills in endoscopic detection of such lesions has been published. Not surprisingly, a follow-up endoscopy after the completion of CRT is considered 'optional' in the National Comprehensive Cancer Network clinical practice guidelines for esophageal cancer.[13] We believe that a reliable endoscopic diagnostic technique is necessary to support a strategy of intense endoscopic follow-ups.

As a cancer referral and research hospital, our institute is unique in its implementation of a vigorous endoscopic follow-up program after primary treatment for all patients with esophageal cancer. Therefore, it is possible to analyze the filed imaging data of endoscopic monitoring on the post-CRT mucosa. In the present study, we aimed to identify useful endoscopic findings through reviewing the image data pool to predict recurrent esophageal cancers limited to the primary site after complete remission (CR) is achieved by CRT.

MATERIALS AND METHODS

Patient population

Between January 2000 and December 2004, 303 patients with esophageal squamous cell carcinoma underwent definitive CRT at the National Cancer Center Hospital East, Kashiwa, Japan. The CRT consisted of 50.4–60 Gy irradiation, together with two cycles of continuous infusion with 5-fluorouracil (5FU) and cisplatin. Up to four courses of CRT were added for those patients who showed a good initial response to treatment.[9]

Table 1 Clinical data of 133 patients achieving complete remission with definitive chemoradiotherapy

Characteristic		Number of patients	%
Sex			
Male		110	82.7
Female		23	17.3
Age (years)			
Mean	62		
Range	39–76		
T stage			
T1		30	22.6
T2		21	15.8
T3		70	52.6
T4		12	9.0
N stage			
N0		46	34.6
N1		87	65.4
M stage			
M0		123	92.5
M1		10	7.5
Clinical stage			
I		16	12.0
II		45	33.8
III		62	46.6
IV		10	7.5
Macroscopic classification			
Type 0		30	22.6
Type 1		19	14.3
Type 2		60	45.1
Type 3		24	18.0

Response to treatment was assessed at the completion of CRT. CR was defined when all the following criteria were met: (i) the disappearance of the tumor lesion or ulcer at the primary site, with negative biopsies; (ii) no esophageal stricture or any condition that prevented a thorough endoscopic examination of the whole esophagus; (iii) no remaining measurable disease or distant metastasis on computer tomography and chest roentgenography; and (5) these criteria were met for at least 4 weeks.

Of the 303 patients, 133 (43.9%) were defined as being in CR at the completion of CRT. Of these 133 patients, 110 were men, with a median age of 62 years. Pretreatment staging of their esophageal cancers was determined with the tumor-node-metastasis classification of the International Union Against Cancer.[14] Seventy (52.6%) patients had T3 tumors; most patients had N1 (65.4%) or M0 (92.5%) disease. Forty-five (33.8%) and 62 (46.6%) patients were classified as clinical stages II and III, respectively (Table 1).

Study design

After achieving CR, initial follow-up endoscopy to confirm CR was scheduled within at most 1–2 months for each patient, accompanied with other necessary studies for the assessment of metastases. After the confirmation of CR, follow-up endoscopy was scheduled every 2–3 months for the first year and every 4–6

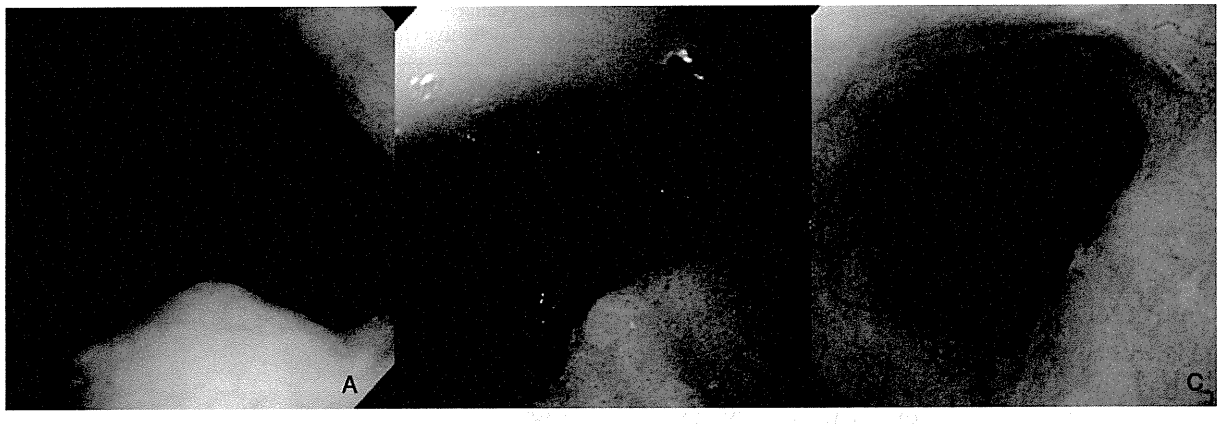

Fig. 1 Initially growing recurrent esophageal cancer at the primary tumor site after complete remission was achieved with chemoradiotherapy may be detected by endoscopy, with features of a submucosal tumor (A), a submucosal tumor with superficial ulcer (B), or a flat erosion (C).

months for 2 years thereafter. Lugol staining and multiple biopsies at the primary site were routinely required.[15] The diagnosis of local recurrence was determined by a positive biopsy.

Of the 133 CR patients, 61 had no recurrence, 56 developed lymph node or distant metastases, and the remaining 16 developed local recurrence at the primary tumor site with no evidence of metastasis. We excluded the 56 patients with lymph node or distant metastases from this study because for them, evaluation of the primary site was not important and only those patients eligible for salvage treatment on local tumors were of interest. Therefore, the endoscopic images of the remaining 77 patients were retrospectively enrolled. This population comprised patients with esophageal squamous cell carcinoma who achieved CR after the initial CRT and developed no metastasis during follow-up, regardless of local recurrence. All of the filed endoscopic images stored after achieving CR, both conventional endoscopy and Lugol-stained chromoendoscopy, were retrospectively collected for reexamination. The stored endoscopic images were evaluated by consensus among three endoscopists experienced in upper gastrointestinal cancer diagnosis (K. T., M. M., K. M.).

RESULTS

Upon the diagnosis of primary-site recurrence for the 16 patients, 13 (81%) had endoscopic findings resembling submucosal tumors (SMT), typically a focal bulge mostly covered by normal-appearing mucosa (Fig. 1A).[16] Eleven of the 13 tumors contained central eroded areas recognized as ulcers or erosions (Fig. 1B and 1C). The remaining three tumors were detected as flat erosions without features of SMT (Table 2).

Images of surveillance endoscopies performed at intervals between CR and the diagnosis of recurrence in the 16 patients were sequentially examined. Newly developed gross lesions at the primary site with negative biopsies were interpreted as recurrent lesions. Evolving lesions were discovered in 13 (81%) patients, including six (38% of the 16 patients) SMT, five (31%) erosions, and two (12%) mild luminal strictures (Table 3).

For all 77 patients achieving CR and free of metastasis, lesions newly developed between CR and the most recent endoscopic surveillance were considered evolving lesions. Therefore, an evolving lesion may be eventually proven to be a recurrence or remain biopsy-negative at the most recent endoscopy. Six of the seven (86%) evolving SMT were subsequently confirmed as recurrent cancer by follow-up

Table 2 Endoscopic findings at primary-site with biopsy-proven recurrence

Endoscopic finding	Number of patients	%
SMT	13	81
SMT with erosion or ulceration	11	
SMT without erosion or ulceration	2	
Erosion	3	19
Total	16	100

SMT, submucosal tumor.

Table 3 Endoscopic findings of newly developed lesion for primary-site recurrent tumors

Preceding newly developed lesions with negative biopsies	Findings at diagnosis of recurrence	Number of patients
SMT	SMT	6
Erosion	SMT	4
Erosion	Erosion	1
Mild stricture	SMT	2
No newly developed lesion	SMT	1
No newly developed lesion	Erosion	2
Total		16

SMT, submucosal tumor.

Table 4 Primary-site biopsy results of the latest surveillance endoscopy for patients who achieved complete remission and remained free of metastasis

Evolving lesion found at preceding endoscopies	Numer of patients (%)	Biopsy result of the latest endoscopy	Number of patients (%)
SMT	7 (9)	Recurrence	6 (86)
		Negative	1 (14)
Erosion	8 (10)	Recurrence	5 (63)
		Negative	3 (37)
Mild stricture	6 (8)	Recurrence	2 (33)
		Negative	4 (67)
No evolving lesion	56 (73)	Recurrence	3 (5)
		Negative	53 (95)
Total	77 (100)		

SMT, submucosal tumor.

endoscopic biopsies. Similarly, five of eight (63%) evolving erosions and two of six (33%) evolving mild strictures were finally confirmed as recurrence. Fifty-six patients were never found to have evolving lesions throughout the follow-up, including three (5%) who were confirmed as recurrence upon the first appearance of an endoscopic lesion. In total, eight of the 21 (38%) patients who developed evolving lesions remained biopsy-negative at their most recent endoscopic follow-up (Table 4).

DISCUSSION

We discovered that the most frequent (81%) endoscopic indicator of primary-site recurrence at its earliest possible stage for a histological diagnosis is SMT. Eighty-one percent of biopsy-proved recurrences were preceded by newly developed lesions such as SMT, erosions, or mild strictures detectable with surveillance endoscopies. Most (86%) evolving SMT with negative biopsies were eventually confirmed as cancer at later endoscopies, but the proportions were lower for other evolving lesions such as erosions (63%) and strictures (33%). This is the first study to describe the morphological changes of early recurring tumors by serial endoscopic observations at short intervals. Our findings will be helpful for improving the skills to detect potentially treatable primary-site recurrence after definitive CRT for esophageal squamous cell carcinoma.

For the endoscopic diagnosis of primary esophageal cancer, several features have been previously described to detect early stage squamous cell carcinoma: localized mucosal erosions in contrast to normal surrounding mucosa; circumscribed mucosal protuberances with irregular configurations; focal areas of mucosal coarsening and congestion; and, rarely, white mucosal plaques.[16] However, these features are not reliable when applied to early recurrent tumors arising from the mucosal bed of a former primary cancer that regressed after CRT. The original esophageal layering and vascular structures have been disrupted by the primary tumor. Furthermore, the expansion and arrangement of recurring neoplastic cells are disrupted by tissue reactions to previous chemotherapy and radiotherapy, as well as by subsequent repair processes. Tumor necrosis, foam cell formation, vascular granulation, inflammatory exudation, and fibrosis are frequent histological sequelae of CRT.[17,18] The minute foci of the initial neoplastic growth may arise from scattered residual cancer cells in deeper tissues, rather than from the superficial mucosal layer, as does the primary cancer.[11] These factors have largely precluded endoscopic ultrasound as a feasible tool in the assessment of residual or recurrent esophageal cancers.[19,20] For the same reason, the endoscopic diagnostic features for recurrent tumors are likely to be different from those for primary tumors.

We speculate that most of the SMT lesions discovered in our study were formed by expanding tumor cells in the submucosal layers, but barely reached the luminal surface because of their depth and constraining fibrosis. Although the overlying mucosa appeared normal, they manifest their first sign by bulging outward. Malignant cells can be captured by biopsy forceps only when they reach the surface in sufficient numbers, or more efficiently, destroy the surface to make an erosion. This might explain why all of the six newly developed SMT yielded negative results at their first biopsies but eventually proved to be recurrences (Table 3).

Several previous studies have aimed to improve the detection of local recurrence by measures other than endoscopy. In addition to pretreatment staging, F-18-fluorodeoxyglucose–positron emission tomography (FDG–PET) is highly sensitive (up to 96%) in detecting recurrent esophageal cancer, but with somewhat lower specificity (68–82%).[21–23] However, its utility in detecting locoregional recurrence is limited by its low specificity (57–75%) for postesophagectomy patients. Postsurgical inflammation and anatomical changes are largely responsible for the false positivity. Detecting small residual or early recurrent cancers is even more challenging because low tumor volume could greatly reduce the sensitivity of FDG–PET. Moreover, such lesions are not distinguishable from post-CRT inflammation or regional lymph-node metastasis.[24,25]

The results of our study disagree with the conventional belief that endoscopy is of limited utility in the management of esophageal cancer after CRT.[13,26] We believe that routine endoscopy, particularly focused on the primary tumor site, is advisable for all patients with esophageal squamous cell carcinoma after the completion of CRT. We also suggest regular endoscopic surveillance at least every three months for those who have achieved CR. The occurrence of

SMT-like lesions after CR is an alarming sign that deserves intensive investigation and follow-up if a modality of salvage treatment is available. Any evolving lesion at the primary site with negative biopsy should be followed closely.

Our retrospective study design has introduced a knowledge bias because the evaluating endoscopists were not totally blinded to the outcomes. Therefore, a randomized controlled trial comparing the clinical outcomes is necessary to establish the role of surveillance endoscopy after definitive CRT for esophageal squamous cell carcinoma.

References

1 Cooper J S, Guo M D, Herskovic A *et al.* Chemoradiotherapy of locally advanced esophageal cancer: long-term follow-up of a prospective randomized trial (RTOG 85-01). JAMA 1999; 81: 1623–7.
2 Suntharalingam M, Moughan J, Coia L R *et al.* The national practice for patients receiving radiation therapy for carcinoma of the esophagus: results of the 1996–1999 Patterns of Care Study. Int J Radiat Oncol Biol Phys 2003; 56: 981–7.
3 Herskovic A, Martz K, al-Sarraf M *et al.* Combined chemotherapy and radiotherapy compared with radiotherapy alone in patients with cancer of the esophagus. N Engl J Med 1992; 326: 1593–8.
4 Kavanagh B, Anscher M, Leopold K *et al.* Patterns of failure following combined modality therapy for esophageal cancer, 1984–90. Int J Radiat Oncol Biol Phys 1992; 24: 633–42.
5 Gill P G, Denham J W, Jamieson G G *et al.* Patterns of treatment failure and prognostic factors associated with the treatment of esophageal carcinoma with chemotherapy and radiotherapy either as sole treatment or followed by surgery. J Clin Oncol 1992; 10: 1037–43.
6 Meunier B, Raoul J, Le Prise E *et al.* Salvage esophagectomy after unsuccessful curative chemoradiotherapy for squamous cell cancer of the esophagus. Dig Surg 1998; 15: 224–6.
7 Swisher S G, Wynn P, Putnam J B *et al.* Salvage esophagectomy for recurrent tumors after definitive chemotherapy and radiotherapy. J Thorac Cardiovasc Surg 2002; 123: 175–83.
8 Nakamura T, Hayashi K, Ota M *et al.* Salvage esophagectomy after definitive chemotherapy and radiotherapy for advanced esophageal cancer. Am J Surg 2004; 188: 261–6.
9 Yano T, Muto M, Minashi K *et al.* Long-term results of salvage endoscopic mucosal resection in patients with local failure after definitive chemoradiotherapy for esophageal squamous cell carcinoma. Endoscopy 2008; 40: 717–21.
10 Yano T, Muto M, Minashi K *et al.* Photodynamic therapy as salvage treatment for local failures after definitive chemoradiotherapy for esophageal cancer. Gastrointest Endosc 2005; 62: 31–6.
11 Mandard A M, Dalibard F, Mandard J C *et al.* Pathologic assessment of tumor regression after preoperative chemoradiotherapy of esophageal carcinoma. Clinicopathologic correlations. Cancer 1994; 73: 2680–6.
12 Brucher B L, Becker K, Lordick F *et al.* The clinical impact of histopathologic response assessment by residual tumor cell quantification in esophageal squamous cell carcinomas. Cancer 2006; 106: 2119–27.
13 Ajani J, Bekaii-Saab T, D'Amico T A *et al.* Esophageal cancer clinical practice guidelines. J Natl Compr Canc Netw 2006; 4: 328–47.
14 Sobin L, Wittekind C. International Union Against Cancer (UICC). TNM Classification of Malignant Tumors, 5th edn. New York: Wiley-Liss, 1997.
15 Mori M, Adachi Y, Matsushima T *et al.* Lugol staining pattern and histology of esophageal lesions. Am J Gastroenterol 1993; 88: 701–5.
16 Silverstein F E, Tytgat G N. Gastrointestinal Endoscopy, 3rd edn. Edinburgh, UK: Mosby, 2002.
17 Darnton S J, Allen S M, Edwards C W *et al.* Histopathological findings in oesophageal carcinoma with and without preoperative chemotherapy. J Clin Pathol 1993; 46: 51–5.
18 Junker K, Thomas M, Schulmann K *et al.* Tumour regression in non-small-cell lung cancer following neoadjuvant therapy. Histological assessment. J Cancer Res Clin Oncol 1997; 123: 469–77.
19 Zuccaro G Jr, Rice T W, Goldblum J *et al.* Endoscopic ultrasound cannot determine suitability for esophagectomy after aggressive chemoradiotherapy for esophageal cancer. Am J Gastroenterol 1999; 94: 906–12.
20 Beseth B D, Bedford R, Isacoff W H *et al.* Endoscopic ultrasound does not accurately assess pathologic stage of esophageal cancer after neoadjuvant chemoradiotherapy. Am Surg 2000; 66: 827–31.
21 Ott K, Weber W, Siewert J R. The importance of PET in the diagnosis and response evaluation of esophageal cancer. Dis Esophagus 2006; 19: 433–42.
22 Flamen P, Lerut A, Van Cutsem E *et al.* The utility of positron emission tomography for the diagnosis and staging of recurrent esophageal cancer. J Thorac Cardiovasc Surg 2000; 120: 1085–92.
23 Kato H, Miyazaki T, Nakajima M *et al.* Value of positron emission tomography in the diagnosis of recurrent esophageal carcinoma. Br J Surg 2004; 91: 1004–9.
24 Nakamura R, Obara T, Katsuragawa S *et al.* Failure in presumption of residual disease by quantification of FDG uptake in esophageal squamous cell carcinoma immediately after radiotherapy. Radiat Med 2002; 4: 181–6.
25 Wieder H A, Brucher B L, Zimermann F *et al.* Time course of tumor metabolic activity during chemoradiotherapy of esophageal squamous cell carcinoma and response to treatment. J Clin Oncol 2004; 22: 900–8.
26 Dittler H J, Fink U, Siewert G R. Response to chemotherapy in esophageal cancer. Endoscopy 1994; 26: 769–71.

Int. J. Radiation Oncology Biol. Phys., Vol. 81, No. 2, pp. 390–396, 2011

0360-3016/$–see front matter

ELSEVIER

doi:10.1016/j.ijrobp.2010.05.027

CLINICAL INVESTIGATION **Prostate**

MULTI-INSTITUTIONAL PHASE II STUDY OF PROTON BEAM THERAPY FOR ORGAN-CONFINED PROSTATE CANCER FOCUSING ON THE INCIDENCE OF LATE RECTAL TOXICITIES

KEIJI NIHEI, M.D., PH.D.,* TAKASHI OGINO, M.D., PH.D.,* MASAKATSU ONOZAWA, M.D.,* SHIGEYUKI MURAYAMA, M.D., PH.D.,† HIROSHI FUJI, M.D., PH.D.,† MASAO MURAKAMI, M.D., PH.D.,‡ AND YOSHIO HISHIKAWA, M.D., PH.D.‡

*Radiation Oncology Division, National Cancer Center Hospital East, Kashiwa, Japan; †Proton Therapy Division, Shizuoka Cancer Center, Shizuoka, Japan; ‡Department of Radiology, Hyogo Ion Beam Medical Center, Hyogo, Japan

Purpose: Proton beam therapy (PBT) is theoretically an excellent modality for external beam radiotherapy, providing an ideal dose distribution. However, it is not clear whether PBT for prostate cancer can clinically control toxicities. The purpose of the present study was to estimate prospectively the incidence of late rectal toxicities after PBT for organ-confined prostate cancer.

Methods and Materials: The major eligibility criteria included clinical Stage T1-T2N0M0; initial prostate-specific antigen level of ≤20 ng/mL and Gleason score ≤7; no hormonal therapy or hormonal therapy within 12 months before registration; and written informed consent. The primary endpoint was the incidence of late Grade 2 or greater rectal toxicity at 2 years. Three institutions in Japan participated in the present study after institutional review board approval from each. PBT was delivered to a total dose of 74 GyE in 37 fractions. The patients were prospectively followed up to collect the data on toxicities using the National Cancer Institute-Common Toxicity Criteria, version 2.0.

Results: Between 2004 and 2007, 151 patients were enrolled in the present study. Of the 151 patients, 75, 49, 9, 17, and 1 had Stage T1c, T2a, T2b, T2c, and T3a, respectively. The Gleason score was 4, 5, 6, and 7 in 5, 15, 80 and 51 patients, respectively. The initial prostate-specific antigen level was <10 or 10–20 ng/mL in 102 and 49 patients, respectively, and 42 patients had received hormonal therapy and 109 had not. The median follow-up period was 43.4 months. Acute Grade 2 rectal and bladder toxicity temporarily developed in 0.7% and 12%, respectively. Of the 147 patients who had been followed up for >2 years, the incidence of late Grade 2 or greater rectal and bladder toxicity was 2.0% (95% confidence interval, 0–4.3%) and 4.1% (95% confidence interval, 0.9–7.3%) at 2 years, respectively.

Conclusion: The results of the present prospective study have revealed a valuable piece of evidence that PBT for localized prostate cancer can achieve a low incidence of late Grade 2 or greater rectal toxicities. © 2011 Elsevier Inc.

Proton beam therapy, Prostate cancer, Radiotherapy, Clinical trial, Rectal toxicity.

INTRODUCTION

The number of patients with organ-confined prostate cancer has been increasing annually because of the widespread screening using prostate-specific antigen (PSA) measurement and aging society. However, organ-confined prostate cancer can now be cured by radical local treatment, including prostatectomy, external beam radiotherapy (EBRT), or brachytherapy, with or without systemic hormonal therapy.

A total dose of >70 Gy using a standard fractionation schedule is considered to be necessary for EBRT to control the disease (1–3); however, the frequency of normal tissue complications increases when the total dose is >70 Gy for conventional EBRT (4, 5). To deliver higher doses to the prostate without increasing the dose to normal tissues, high-technology EBRT, such as three-dimensional conformal radiotherapy (3D-CRT), intensity-modulated radiotherapy (IMRT), and particle therapy have been developed and

Reprint requests to: Keiji Nihei, M.D., Ph.D., Radiation Oncology Division, National Cancer Center Hospital East, 6-5-1 Kashiwanoha, Kashiwa 277-8577 Japan. Tel: (+81) 4-7133-1111; Fax: (+81) 4-7131-4724; E-mail: knihei@east.ncc.go.jp

Presented in part at the 51st Annual Meeting of the American Society for Therapeutic Radiology and Oncology, September 21–25, 2008, Boston, MA; and at the 48th Meeting of the Particle Therapy Cooperative Group, October 1–3, 2009, Heidelberg, Germany.

Supported in part by the Foundation for the Promotion of Cancer Research in Japan.

Conflict of interest: none.

Received Feb 26, 2010, and in revised form April 30, 2010. Accepted for publication May 14, 2010.

used for more than one decade. Although high-technology techniques of EBRT using X-rays such as 3D-CRT and IMRT have been prospectively evaluated (6–9), the amount of prospective information on the use of proton beam therapy (PBT) alone is limited.

The proton beams used in the modality of particle therapy have distinct physical advantages over conventional photon beams. Proton beams have a low entrance dose, a maximal dose at any prescribed depth called the "Bragg peak," and no exit dose. The "Bragg peak" can be spread out and shaped to conform to the depth and volume of an irregular target. PBT can thus create an inherently three-dimensional conformal dose distribution without exposure of the surrounding normal tissues to excessive doses as compared with the case in conformal photon treatment.

PBT for prostate cancer allows a good dose distribution to be obtained using simple bilateral opposed fields, without exposure of the rectum and bladder to excessive doses. Thus, PBT is theoretically an excellent therapeutic modality owing to its efficacy with reduced toxicity to normal tissues. However, because of the lack of prospective data, it is not yet clear whether PBT can control the incidence of toxicity in the clinical setting. With this background, we started a multi-institutional Phase II trial for patients with organ-confined prostate cancer, focusing on the incidence of late Grade 2 or greater rectal toxicity.

METHODS AND MATERIALS

Patients

The eligibility criteria for inclusion of patients in the present study were (*1*) histologically proven prostate adenocarcinoma, (*2*) clinical Stage II disease (2002 TNM classification, 6th edition, cT1-T2N0M0), (*3*) an initial PSA level of ≤20 ng/mL and Gleason score (GS) of ≤7, (*4*) no history of hormonal therapy or hormonal therapy within 12 months before registration, (*5*) performance status (Eastern Cooperative Oncology Group) 0–2, (*6*) preserved organ function, (*7*) no other active malignancy, and (*8*) written informed consent. Patients with a GS of <7 and PSA level of <10 ng/mL and those with a GS of 7 and/or a PSA level of >10 ng/mL were defined as the low- and intermediate-risk groups, respectively. Patients with Stage cT3-T4, GS 8–10, and/or PSA >20 were not eligible for the present study.

Study endpoints

The primary endpoint was the incidence of late Grade 2 or greater rectal toxicity at 2 years. The secondary endpoints included other toxicities (both acute and late), biochemical relapse-free survival, overall survival, and disease-specific survival. Biochemical failure in the present study was defined as a PSA value of nadir plus 2.0 ng/mL (10, 11), the initiation of any hormonal therapy, or death from any cause.

Study design and statistical analysis

A multi-institutional Phase II study was planned for prospective collection of the toxicity data. The sample size was calculated by the interval estimation method to maintain the accuracy of estimation, using 95% confidence intervals (CIs) of the primary endpoint. The expectation value of the primary endpoint has been defined as <10% according to previous reports of EBRT (12–16). The study sample size was calculated as 150 patients, such that the upper limit of the 95% CI of the primary endpoint was <16% when the actual incidence was <10%. The planned accrual period was 2 years.

Participating institutions

Five institutions were equipped to provide PBT at the beginning of the present study in Japan; three of them participated in the present study, and the institutional review board at each of the three institutions approved the present study (National Cancer Center Hospital East, Kashiwa; Shizuoka Cancer Center, Shizuoka; and Hyogo Ion Beam Medical Center, Hyogo).

Treatment planning

The patients were placed in the supine position and fixed with a vacuum cushion or a thermoplastic cast. The patients were instructed to maintain regular bowel movement; patients with constipation were prescribed laxatives such as magnesium oxide, sennoside, and/or picosulfate sodium to control bowel movement. The bladder filling was controlled by water drinking after urination, and all PBT sessions were performed with a full bladder.

The clinical target volume was defined as the prostate alone for low-risk patients and as the prostate plus the proximal seminal vesicles for intermediate-risk patients, at least encompassing all-known diseases identified by the planning computed tomography scan and other clinical information. The planning target volume consisted of the clinical target volume with optimal margins to account for the uncertainties from the patient setup or internal organ motion, which were estimated at each institution (Table 1). The rectum, from the sigmoid flexure to the anal verge, and the entire bladder as solid organs were delineated as the critical normal structures.

Proton beam therapy

The PBT was delivered at a total dose of 74 GyE in 37 fractions (2 GyE/d). In the low-risk patients, the prostate alone received 74 GyE; in the intermediate-risk patients, a booster dose of 24 GyE was added to the prostate alone after the initial 50 GyE was delivered to the prostate and proximal seminal vesicles. As listed in Table 1, the dose prescription was determined by each institutional method. The dose constraints for the normal tissues were as follows, on the basis of the results from our previous analysis (17) (V_X indicates the percentage of volume receiving more than x GyE): rectum, V_{50} <35%, V_{60} <25%, and V_{70} <15% in the low-risk patients; V_{50} <40%, V_{60} <30%, and V_{70} <20% in the intermediate-risk patients; bladder, V_{65} <50%, V_{70} <35%; femoral head, maximal dose <50 GyE.

Table 1. Details of treatment planning in each institution

Institution	PTV margin (mm)	Dose prescription	Bolus/collimator
NCCHE	7	90% dose to PTV	Individual bolus/ collimator
SCC	5	95% dose to PTV	Individual bolus/ collimator
HIBMC	8–10	To isocenter	No bolus/multileaf collimator

Abbreviations: NCCHE = national cancer center hospital east; SCC = shizuoka cancer center; HIBMC = hyogo ion beam medical center; PTV = planning target volume.

Bilateral opposed fields were used for proton dose delivery. The range modulation by bar-ridge filters was used to generate a spread-out Bragg peak. Proton beams with optimal energy in the range of 190–235 MeV were selected, and individual boluses and collimators were manipulated to conform to the target volume. Daily verification of patient positioning was performed in all patients using orthogonal radiography according to the bony structures. The relative biologic effectiveness of the proton beam was estimated to be 1.1 compared with that of the photon X-rays (GyE = proton Gy × 1.1), in animal experiment conducted at each institution.

Assessments

The registered patients were prospectively followed up to collect data on the toxicities and PSA values at 1 month and once every 3 months after PBT completion for the first 2 years and once every 6 months thereafter.

Late toxicities were defined as those observed >90 days after the start of PBT, but the Radiation Therapy Oncology Group (RTOG)/European Organization for Research and Treatment of Cancer late radiation morbidity scoring scheme was not used in the present study to assess the late toxicities. Instead, so that the observed symptoms could be individually assessed and scored objectively, the National Cancer Institute Common Toxicity Criteria, version 2.0, was used to assess the acute and late toxicities. The symptoms of rectal and/or bladder toxicities assessed in the present study included proctitis, rectal bleeding, rectal pain, hematuria, urinary frequency/urgency, urinary retention, and dysuria (painful urination). Toxicity grading was determined using the severity of each symptom assessed objectively. The Common Terminology Criteria for Adverse Events, version 3.0, was not available when preparing the present study and was not used.

The cumulative incidence of the toxicities and the survival rates were analyzed using the Kaplan-Meier method.

RESULTS

Patients

Between March 2004 and March 2007, 151 patients were enrolled at the 3 institutions for the present study. The patient characteristics are listed in Table 2. Of the 151 patients, 77 and 74 were low- and intermediate-risk, respectively. All the patients enrolled in the present study received the planned PBT up to a dose of 74 GyE in 37 fractions. The median follow-up period was 43.4 months (range, 3–62). Of the 151 patients, 3 were lost to follow-up within the first 2 years, and 1 patient died of other causes on Day 165, without biochemical failure. These 4 patients were excluded from the analysis of late toxicity. All the patients enrolled in the present study were included in the assessment of the acute toxicities and efficacy.

Acute toxicities

The acute rectal and bladder toxicities observed within 90 days of the initiation of PBT are listed in Table 3. All the acute toxicities observed were transient and resolved spontaneously after completion of PBT. No Grade 3 or greater acute toxicities were observed. The rectal toxicities observed included anal pain at defecation, soft stool, anal discomfort, and rectal bleeding. The bladder toxicities were urinary frequency, dysuria, narrow stream, and urinary retention.

Table 2. Patient and tumor characteristics

Characteristic	Value
All patients (*n*)	151
Age (y)	
Median	67
Range	51–82
cT Stage (*n*)	
T1c	75
T2a	49
T2b	9
T2c	17
T3a	1
Gleason score (*n*)	
4	5
5	15
6	80
7	51
iPSA (ng/mL)	
10	102
10–20	49
Hormonal therapy (*n*)	
Yes	42
No	109
Risk group (*n*)	
Low risk	77
Intermediate risk	74

Abbreviation: iPSA = initial prostate-specific antigen.

Late toxicities

The late toxicities at the final follow-up of the 147 patients who had been followed up for >2 years are listed in Table 4. No Grade 3 or greater late rectal toxicities were observed. The late rectal toxicities observed included rectal bleeding, urgency of defecation, and anal pain. The bladder toxicities were transient gross hematuria and urinary retention.

The Kaplan-Meier curves of late rectal and bladder toxicities are shown in Fig. 1. The incidence of late Grade 2 or greater rectal toxicity was 2.0% (95% CI, 0–4.3%) at 2 years (primary endpoint of the present study) and 4.1% (95% CI, 0.4–7.7%) at the final follow-up. The corresponding data for bladder toxicity were 4.1% (95% CI, 0.9–7.3%) at 2 years and 7.8% (95% CI, 2.9–12.8%) at the final follow-up.

Efficacy

The median follow-up period was 43.4 months in the present study. We evaluated the biochemical relapse-free survival

Table 3. Acute toxicities

Toxicity	Patients (*n*)
Total	151 (100)
Rectum	
Grade 0	135 (89)
Grade 1	15 (10)
Grade 2	1 (0.7)
Bladder	
Grade 0	46 (30)
Grade 1	87 (58)
Grade 2	18 (12)

Data in parentheses are percentages.

Table 4. Late toxicities

Toxicity	Patients (*n*)
Total	147* (100)
Rectum	
Grade 0	115 (78)
Grade 1	27 (18)
Grade 2	5 (3)
Bladder	
Grade 0	128 (87)
Grade 1	9 (6)
Grade 2	8 (5)
Grade 3	2 (1)

Data in parentheses are percentages.
* Number of patients followed up for >2 years.

using the failure definition of nadir plus 2.0 ng/mL; the Kaplan-Meier curve is shown in Fig. 2. Two patients died of other causes on Day 165 and Day 1,202, respectively, without biochemical failure. No patients died of prostate cancer. The biochemical relapse-free survival rate was 94% at 3 years (95% CI, 90–98%).

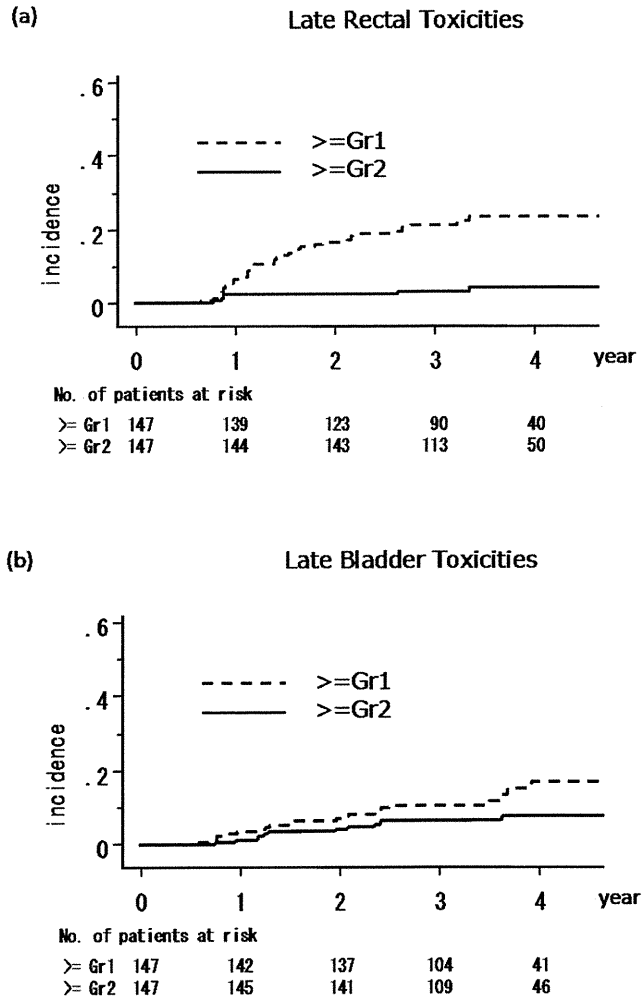

Fig. 1. Kaplan-Meier curves of late (a) rectal and (b) bladder toxicity. Gr = grade.

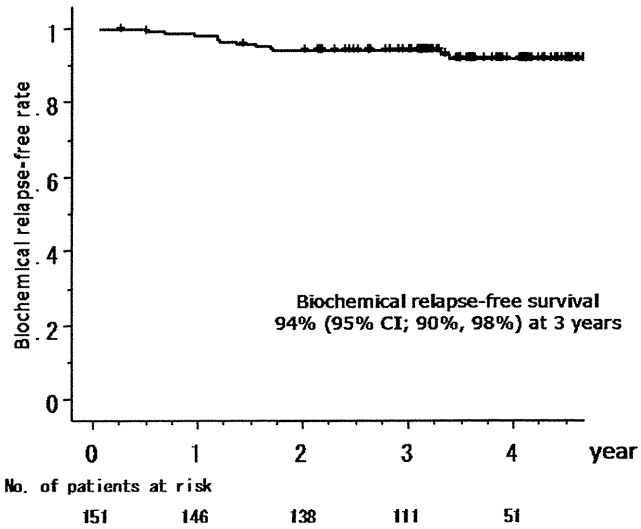

Fig. 2. Biochemical relapse-free survival using definition of nadir plus 2.0 ng/mL. CI = confidence interval.

DISCUSSION

The results of the present prospective study have provided valuable evidence to show a low incidence of late Grade 2 or greater rectal toxicities after PBT for organ-confined prostate cancer. Although PBT is theoretically an excellent modality for EBRT, providing an ideal dose distribution, few well-designed prospective clinical trials are available to corroborate its superiority. The present prospective study was conducted with the aim of scientifically clarifying whether PBT can control the incidence of late rectal toxicity.

The RTOG conducted a Phase I-II dose-escalation study to determine the maximal tolerated dose of 3D-CRT for prostate cancer (RTOG 94-06). The toxicity results of RTOG 94-06 showed a significantly lower incidence of Grade 3 or greater late toxicity but a significantly greater incidence of Grade 2 or less late toxicity than expected from the results of previous RTOG trials (13–15, 18). Although Grade 2 toxicity is generally defined as moderate in severity and is often underestimated, the patients' quality of life can suffer even from such moderate toxicity. Therefore, it is becoming increasingly important to devise sophisticated techniques for high-dose EBRT, such that even the frequency of moderate Grade 2 or less toxicity can be reduced in patients with prostate cancer.

Of the late toxicities that characteristically occur in patients receiving high-dose EBRT for prostate cancer are rectal toxicities, which in most cases, are represented by rectal bleeding, occurring within 2 years of treatment completion. For this reason, the primary endpoint of the present study was defined as the incidence of late Grade 2 or greater rectal toxicity at 2 years after treatment completion.

Since the 1990s, when the existence of a dose–response relationship was suggested in prostate cancer patients undergoing EBRT, dose escalation has been eagerly pursued using high-technology EBRT. In a randomized Phase III trial of 3D-CRT at the M.D. Anderson Cancer Center, the toxicity results revealed an incidence of late Grade 2 or greater

gastrointestinal (GI) toxicity in a high-dose arm (78 Gy in 39 fractions) and standard-dose arm (70 Gy in 35 fractions) of 26% and 12%, respectively (16). Michalski *et al.* conducted a multi-institutional dose-escalation Phase I-II study of 3D-CRT (RTOG 9406; Level 1, 2, and 3, 68.4, 73.8, and 79.2 Gy at 1.8 Gy/fraction; Level 4 and 5, 74 and 78 Gy in 2 Gy/fraction, respectively) and reported the late toxicity profiles at each dose level. Late Grade 2 or greater GI toxicity occurred in 9–13%, 7–9%, 11–14%, 10–16%, and 25–26%, respectively, at dose levels 1–5 (6).

Intensity-modulated RT (IMRT) is a modality of high-technology EBRT. The Memorial Sloan-Kettering Cancer Center has been conducting a single-institutional dose-escalation trial of 3D-CRT and IMRT. Zelefsky *et al.* (7–9) reported that Grade 2 or greater late GI toxicity occurred at an incidence of 16% in patients who had undergone 3D-CRT to a total dose of 75.6–81 Gy (1.8 Gy/fraction). The corresponding incidence was only 2%, even in patients who had undergone IMRT to a total dose of 81–86.4 Gy (7–9). According to a retrospective analysis from the Fox Chase Cancer Center, Grade 2 or greater late GI toxicity occurred at an incidence of 2.4% in patients who had undergone IMRT to a total dose of 74–78 Gy (2 Gy/fraction) (19). However, in some reports, no reduction in the incidence of late toxicity could be achieved despite using IMRT. De Meerleer *et al.* (20) reported that 18% of patients experienced Grade 2 or greater late GI toxicity after receiving a total dose of 74–76 Gy (2 Gy/fractions). Vora *et al.* (21) also reported an incidence of late Grade 2 or greater toxicity of 24% in patients who had undergone IMRT to a total dose of 75.6 Gy.

The PBT facility was installed at Loma Linda University Medical Center in 1990, and the morbidity results for the prostate cancer patients treated to a total dose of 74–75 GyE (1.8–2.0 GyE/fraction) were reported. Late Grade 2 GI toxicity had developed in 21% of the patients at 3 years after treatment completion (22).

The toxicity results in previous reports are summarized in Table 5. The incidence of late Grade 2 or greater rectal toxicity in patients who had undergone 3D-CRT was 9–16% (6, 8). The Memorial Sloan-Kettering Cancer Center and Fox Chase Cancer Center reported a very low incidence of late Grade 2 or greater rectal toxicity (2–2.4%) in patients who had undergone IMRT (7, 9, 19). In contrast, some other centers have reported a high incidence of late rectal toxicity (>15%) even in patients who had undergone IMRT (20, 21). Our results have shown that the incidence of late Grade 2 or greater rectal toxicity was 2.0% at 2 years and 4.1% at the final follow-up; the upper limit of the 95% CIs of these values was 4.3% and 7.7%, respectively. Our results cannot be directly compared with the toxicity data from previous reports, because these studies used different grading scales and also included retrospective and/or single institution-specific data. However, the incidence of late rectal toxicity associated with PBT in the present study was lower than those from the 3D-CRT series and, at least, was not greater than the historical data on the incidence of late Grade 2 or greater GI toxicity after 3D-CRT and IMRT (12–16). The result for the primary endpoint in the present study was 2.0% (95% CI, 0–4.3%) at 2 years, providing at least one piece of scientific evidence of PBT in patients with prostate cancer.

Table 5. Overview of late gastrointestinal toxicity in EBRT for localized prostate cancer

Institution/study	Patients (*n*)	Dose (Gy)	Technique	Grading scale	Grade 1	Grade 2	Grade 3	Follow-up (y)
MDACC (16)	150	70	3D-CRT	RTOG/LENT	36%	11%	1%	6
	151	78			28%	19%	7%	6
					23%, Grade 2/3			2
RTOG 9406 (6)	112	68.4	3D-CRT	RTOG	9-13%, Grade 2/3			9–12
	300	73.8			7-9%, Grade 2/3			7–10
	167	79.2			11-14%, Grade 2/3			9
	256	74			10-16%, Grade 2/3			7–8
	220	78			25-26%, Grade 2/3			6
MSKCC (7–9)	695	75.6–81	3D-CRT	Modified RTOG/CTCAE,	16%, Grade 2/3			5
	561	81–86.4	IMRT	version 3.0	2%, Grade 2/3			7
FCCC (19)	216	74–78	IMRT	Modified RTOG/LENT	2.4%, Grade 2/3			3.5
Ghent University (20)	133	74–76	IMRT	Modified RTOG	47%	17%	1%	3
Mayo Clinic Arizona (21)	145	75.6	IMRT	Modified RTOG	20%	23%	1%	4
LLUMC (22)	643	74	PBT alone	RTOG	—	21%	—	3
		75	X+PBT					
Present study	151	74	PBT alone	NCI-CTC, version 2.0	14%	2.0%, Grade 2/3		2

Abbreviations: EBRT = external beam radiotherapy; MDACC = M.D. Anderson Cancer Center; 3D-CRT, three-dimensional conformal radiotherapy; RTOG = radiation therapy oncology group; LENT = late effects normal tissue task force; MSKCC = memorial sloan-kettering cancer center; IMRT = intensity-modulated radiotherapy; CTCAE = common terminology criteria for adverse events; FCCC = fox chase cancer center; LLUMC = loma linda university medical center; X = photon radiotherapy; PBT = proton beam therapy; NCI-CTC = national cancer institute common toxicity criteria.

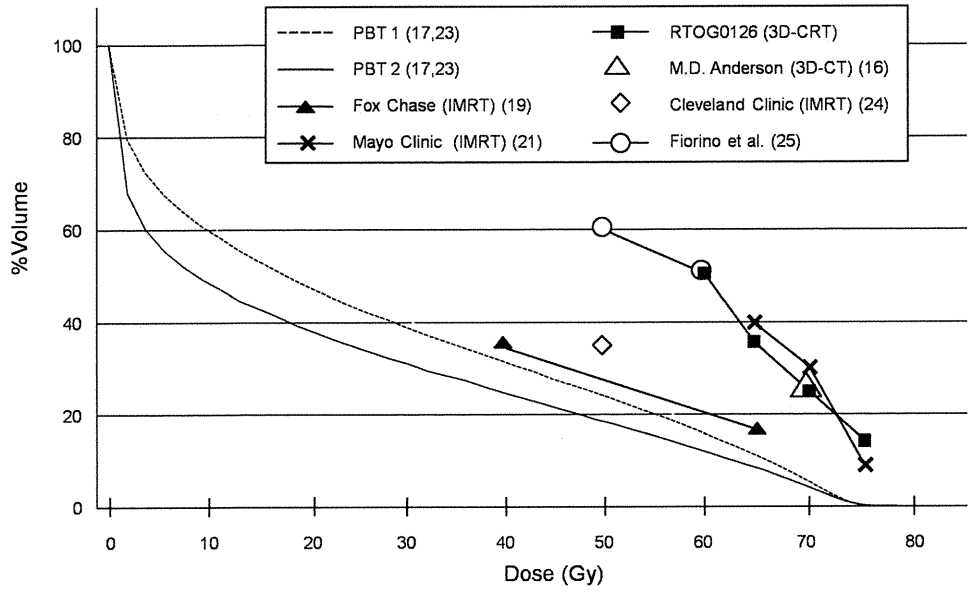

Fig. 3. Average dose–volume histograms (DVHs) for rectum in photon beam therapy (PBT) compared with other dose constraints used in three-dimensional conformal radiotherapy (3D-CRT) or intensity-modulated radiotherapy (IMRT). PBT1 = PBT for intermediate-risk patients; PBT2 = PBT for low-risk patients; RTOG = Radiation Therapy Oncology Group. Data in parentheses indicate reference report.

The previously reported average dose–volume histograms for the rectum in PBT performed at National Cancer Center Hospital East are shown in Fig. 3 (17, 23) and were compared with the other dose constraints used in 3D-CRT or IMRT (16, 19, 21, 24, 25). PBT with simple bilateral opposed fields can thus reduce the dose to the rectum through high to intermediate dose levels, thereby achieving the ideal dose–volume histogram for the rectum. Although bilateral opposed fields can present another issue regarding the dose to the femoral head, the maximal dose to the femoral head in PBT with simple bilateral opposed fields is <35 GyE (45% of the prescribed dose), and V_{30} of the femoral head is <40%.

The total dose of PBT used in the present study was 74 GyE, administered using a conventional fractionation schema (2 GyE/fractions); however, the possible benefit of additional dose escalation and hypofractionation of EBRT for prostate cancer has been suggested, and the efficacy of such a strategy is now under investigation in some randomized trials (16, 26–28). As shown in Fig. 3, the excellent dose–volume histograms for the rectum in PBT might allow the implementation of these strategies; however, additional prospective data are required to ascertain whether PBT administered using these investigational approaches can yield a low frequency of late rectal toxicity.

A more objective grading scale might be necessary to allow comparison of the morbidity data, because different grading scales have been used in previous reports. Thus, the health-related quality of life might be a more rigid and comparable indicator for assessing the toxicities.

Late genitourinary toxicity often occurs after a longer follow-up period (29, 30) and is another issue that needs to be addressed with the use of high-dose EBRT for prostate cancer. As shown in Fig. 1, the incidence curve of late bladder toxicity seems to have been increasing over the years, and that of late rectal toxicity reached a plateau after a few years. Longer follow-up is needed for a more precise assessment of both late genitourinary and GI toxicity.

Quality assurance procedures for clinical assessments have an important role in enhancing confidence in the results of multi-institutional clinical trials. At the beginning of the present study, the specifications for PBT facilities differed among the participating institutions, and the method of delivery of the proton beams to the target organs was defined at the discretion of each institution (Table 1). Although such institutional differences in the method of dose delivery can affect the incidence of toxicity, no significant difference was found in the incidence of toxicity among the three institutions in the present study. Owing to the increasing number of PBT facilities, implementation of quality assurance procedures for PBT in multi-institutional trials, from both the clinical and the physics aspect, is gaining importance.

REFERENCES

1. Perez CA, Walz BJ, Zivnuska FR, *et al.* Irradiation of carcinoma of the prostate localized to the pelvis: Analysis of tumor response and prognosis. *Int J Radiat Oncol Biol Phys* 1980;6:555–563.

2. Hanks GE, Martz KL, Diamond JJ. The effect of dose on local control of prostate cancer. *Int J Radiat Oncol Biol Phys* 1988; 15:1299–1305.

3. Kupelian PA, Elshaikh M, Reddy CA, *et al.* Comparison of the efficacy of local therapies for localized prostate cancer in the prostate-specific antigen era: A large single-institution experience with radical prostatectomy and external-beam radiotherapy. *J Clin Oncol* 2002;20:3376–3385.
4. Pilepich MV, Krall JM, Sause WT, *et al.* Prognostic factors in carcinoma of the prostate—Analysis of RTOG study 75-06. *Int J Radiat Oncol Biol Phys* 1987;13:339–349.
5. Hanks GE. External-beam radiation therapy for clinically localized prostate cancer: Patterns of care studies in the United States. *NCI Monogr* 1988;7:75–84.
6. Michalski JM, Bae K, Roach M, *et al.* Long-term toxicity following 3D conformal radiation therapy for prostate cancer from the RTOG 9406 phase I/II dose escalation study. *Int J Radiat Oncol Biol Phys* 2010;76:14–22.
7. Cahlon O, Hunt M, Zelefsky MJ. Intensity-modulated radiation therapy: Supportive data for prostate cancer. *Semin Radiat Oncol* 2008;18:48–57.
8. Zelefsky MJ, Levin EJ, Hunt M, *et al.* Incidence of late rectal and urinary toxicities after three-dimensional conformal radiotherapy and intensity-modulated radiotherapy for localized prostate cancer. *Int J Radiat Oncol Biol Phys* 2008;70:1124–1129.
9. Zelefsky MJ, Chan H, Hunt M, *et al.* Long-term outcome of high dose intensity modulated radiation therapy for patients with clinically localized prostate cancer. *J Urol* 2006;176: 1415–1419.
10. Roach M III, Hanks G, Thames H Jr., *et al.* Defining biochemical failure following radiotherapy with or without hormonal therapy in men with clinically localized prostate cancer: Recommendations of the RTOG-ASTRO Phoenix consensus conference. *Int J Radiat Oncol Biol Phys* 2006;65:965–974.
11. Thames H, Kuban D, Levy L, *et al.* Comparison of alternative biochemical failure definitions based on clinical outcome in 4839 prostate cancer patients treated by external beam radiotherapy between 1986 and 1995. *Int J Radiat Oncol Biol Phys* 2003;57:929–943.
12. Zelefsky MJ, Fuks Z, Hunt M, *et al.* High-dose intensity modulated radiation therapy for prostate cancer: Early toxicity and biochemical outcome in 772 patients. *Int J Radiat Oncol Biol Phys* 2002;53:1111–1116.
13. Michalski JM, Purdy JA, Winter K, *et al.* Preliminary report of toxicity following 3D radiation therapy for prostate cancer on 3DOG/RTOG 9406. *Int J Radiat Oncol Biol Phys* 2000;46: 391–402.
14. Ryu JK, Winter K, Michalski JM, *et al.* Interim report of toxicity from 3D conformal radiation therapy (3D-CRT) for prostate cancer on 3DOG/RTOG 9406, level III (79.2 Gy). *Int J Radiat Oncol Biol Phys* 2002;54:1036–1046.
15. Michalski JM, Winter K, Purdy JA, *et al.* Preliminary evaluation of low-grade toxicity with conformal radiation therapy for prostate cancer on RTOG 9406 dose level I and II. *Int J Radiat Oncol Biol Phys* 2003;56:192–198.
16. Pollack A, Zagars GK, Starkschall, *et al.* Prostate cancer radiation dose response: Results of the M.D. Anderson phase III randomized trial. *Int J Radiat Oncol Biol Phys* 2002;53:1097–1105.
17. Nihei K, Ogino T, Ishikura S, *et al.* Phase II feasibility study of high-dose radiotherapy for prostate cancer using proton boost therapy: First clinical trial of proton beam therapy for prostate cancer in Japan. *Jpn J Clin Oncol* 2005;35:745–752.
18. Michalski JM, Winter K, Purdy JA, *et al.* Trade-off to low-grade toxicity with conformal radiation therapy for prostate cancer on Radiation Therapy Oncology Group 9406. *Semin Radiat Oncol* 2002;12(Suppl. 1):75–80.
19. Eade TN, Horwitz EM, Ruth K, *et al.* A Comparison of acute and chronic toxicity for men with low-risk prostate cancer treated with intensity-modulated radiation therapy or I 125 permanent implant. *Int J Radiat Oncol Biol Phys* 2008;71:338–345.
20. De Meerleer GO, Fonteyne VH, Vakaet L, *et al.* Intensity-modulated radiation therapy for prostate cancer: Late morbidity and results on biochemical control. *Radiother Oncol* 2007;82:160–166.
21. Vora SA, Wong WW, Schild SE, *et al.* Analysis of biochemical control and prognostic factors in patients treated with either low-dose three dimensional conformal radiation therapy or high-dose intensity-modulated radiotherapy for localized prostate cancer. *Int J Radiat Oncol Biol Phys* 2007;68:1053–1058.
22. Slater JD, Yonemoto LT, Rossi CJ Jr., *et al.* Conformal proton therapy for prostate cancer. *Int J Radiat Oncol Biol Phys* 1998; 42:299–304.
23. Nihei K, Nishio T, Ishikura S, *et al.* Analysis of dose volume histograms in proton therapy for prostate cancer (ECCO [European Cancer Organisation] 12 Abstract Book). *Eur J Cancer Suppl* 2003;1:S161–S162.
24. Kupelian PA, Reddy CA, Klein EA, *et al.* Short-course intensity-modulated radiotherapy (70 Gy at 2.5 Gy per fraction) for localized prostate cancer: Preliminary results on late toxicity and quality of life. *Int J Radiat Oncol Biol Phys* 2001;51:988–993.
25. Fiorino C, Cozzarini C, Vavassori V, *et al.* Relationships between DVHs and late rectal bleeding after radiotherapy for prostate cancer: Analysis of a large group of patients pooled from three institutions. *Radiother Oncol* 2002;64:1–12.
26. Fowler JF, Ritter MA, Chappell RJ, *et al.* What hypofractionated protocols should be tested for prostate cancer? *Int J Radiat Oncol Biol Phys* 2003;56:1093–1104.
27. Kupelian PA, Thakkar VV, Khuntia D, *et al.* Hypofractionated intensity-modulated radiotherapy (70 Gy at 2.5 Gy per fraction) for localized prostate cancer: Long-term outcomes. *Int J Radiat Oncol Biol Phys* 2005;63:1463–1468.
28. Zietman AL, DeSilvio ML, Slater JD, *et al.* Comparison of conventional-dose vs high-dose conformal radiation therapy in clinically localized adenocarcinoma of the prostate: A randomized controlled trial. *JAMA* 2005;294:1233–1240.
29. Gardner BG, Zeitman AL, Shipley WU, *et al.* Late normal tissue sequelae in the second decade after high dose radiation therapy with combined photons and conformal protons for locally advanced prostate cancer. *J Urol* 2002;167:123–126.
30. Lawton CA, Bae K, Pilepich M, *et al.* Long-term treatment sequelae after external beam irradiation with or without hormonal manipulation for adenocarcinoma of the prostate: Analysis of Radiation Therapy Oncology Group studies 85-31, 86-10, and 92-02. *Int J Radiat Oncol Biol Phys* 2008;70:437–441.